Appl Biochem Biotechnol (2010) 160:1341–1355
DOI 10.1007/s12010-009-8636-6

Alpha-Glucosidase Folding During Urea Denaturation: Enzyme Kinetics and Computational Prediction

Xue-Qiang Wu · Jun Wang · Zhi-Rong Lü · Hong-Min Tang · Daeui Park · Sang-Ho Oh · Jong Bhak · Long Shi · Yong-Doo Park · Fei Zou

Received: 5 January 2009 / Accepted: 1 April 2009 /
Published online: 6 May 2009

Abstract In this study, we investigated structural changes in alpha-glucosidase during urea denaturation. Alpha-glucosidase was inactivated by urea in a dose-dependent manner. The inactivation was a first-order reaction with a monophase process. Urea inhibited alpha-glucosidase in a mixed-type reaction. We found that an increase in the hydrophobic surface of this enzyme induced by urea resulted in aggregation caused by unstable folding intermediates. We also simulated the docking between alpha-glucosidase and urea. The docking simulation suggested that several residues, namely THR9, TRP14, LYS15, THR287, ALA289, ASP338, SER339, and TRP340, interact with urea. Our study provides insights into the alpha-glucosidase unfolding pathway and 3D structure of alpha-glucosidase.

Keywords Alpha-glucosidase · Urea unfolding · Docking simulation

Abbreviations
pNPG *p*-Nitrophenyl α-D-glucopyranoside
pNP 4-Nitrophenol

Xue-Qiang Wu and Jun Wang have contributed equally to this study.

X.-Q. Wu · Z.-R. Lü · L. Shi · Y.-D. Park · F. Zou (✉)
Department of Environmental Health, School of Public Health and Tropical Medicine,
Southern Medical University, Baiyun District, North of Guangzhou Road No.1838, Guangzhou 510515,
People's Republic of China
e-mail: zoufei_dean@hotmail.com

J. Wang
School of Medicine, Shenzhen University, Shenzhen 518060, People's Republic of China

H.-M. Tang · Y.-D. Park
Yangtze Delta Region Institute of Tsinghua University, Jiaxing 314050, People's Republic of China

D. Park · S.-H. Oh · J. Bhak
Korean BioInformation Center (KOBIC), KRIBB, Daejeon 305-806, South Korea

SDS Sodium dodecyl sulfate
ANS 1-Anilino-8-naphthalenesulfonate

Introduction

Alpha-glucosidase (α-D-glucoside glucohydrolase, EC 3.2.1.20), otherwise known as MAL12 or maltase, is encoded by the MAL1 complex locus. This inducible enzyme is involved in maltose catabolism; it catalyzes the hydrolysis of terminal α-(1-4)-linked D-glucose residues from the nonreducing end of alpha-glucoside [1]. In addition, alpha-glucosidase has broad substrate specificity and can hydrolyze a variety of glucopyranosides such as sucrose, trehalose, and maltose. Furthermore, alpha-glucosidase is a member of the α-amylase family; proteins in this family are characterized by a common (β/α) 8-barrel fold and a common catalytic reaction mechanism [2–4].

In industry, alpha-glucosidase is used to convert starch to fermentable sugars—an important step in alcohol production. In contrast, in a clinical setting, alpha-glucosidase inhibition is monitored closely in diabetic patients, as this enzyme is involved in sugar metabolism. Alpha-glucosidase inhibitors are oral anti-diabetic drugs used to treat diabetes mellitus type 2 and function by preventing the digestion of carbohydrates [5–7]. These inhibitors are used to establish greater glycemic control over hyperglycemia in diabetes mellitus type 2 patients, particularly with regard to postprandial hyperglycemia. However, few studies have focused on conformational and activity changes in this enzyme.

In vitro protein denaturation studies have provided insight into how enzyme structure is related to catalysis and stability, including the forces required to maintain tertiary structure, conformational flexibility, compactness, and the folding pathway. The most frequently applied denaturant to study protein folding is urea; it is used to probe structural characteristics of enzymes. Although urea has been shown to function via different mechanisms depending on the protein fold, the detailed mode of interaction between proteins and urea is unclear. Urea preferentially interacts with nonpolar and substituent groups, regardless of polarity height. Polar or nonpolar interactions between urea and polar groups of amides and peptides provide the driving force for the destabilization of proteins [8]. As an ionic molecule, urea at a high concentration has a strong destabilizing effect on polar interactions in protein structures. In a previous study, urea interacted favorably with both nonpolar and polar surfaces and weakened both hydrophobic interactions in proteins and intramolecular hydrogen bonds [9]. In the clinic, physicians have attempted to use urea to treat psoriasis [10, 11], and urea has been used to increase the permeability of skin to drugs and water [12–15].

Urea has been used to characterize active site properties in both transient and equilibrium states of folding pathways of various enzymes. Here, we conducted a real-time analysis as well as an equilibrium kinetic unfolding study of alpha-glucosidase in the presence of urea denaturant to expand our understanding of the 3D structure of alpha-glucosidase. Our results show that alpha-glucosidase reacts differently to different urea concentrations and has unstable folding intermediates, which can induce aggregation in the folding pathway. Kinetic rate constants and other parameters were calculated and the putative unfolding pathway for alpha-glucosidase is discussed. Probing and characterization of conformational intermediates during polypeptide folding is an important goal of protein research. Our urea-based folding study of alpha-glucosidase provides novel insights into the structure and inhibition of this important enzyme.

Materials and Methods

Materials

Alpha-glucosidase (*Saccharomyces cerevisiae*), *p*-nitrophenyl α-D-glucopyranoside, 1-anilino-8-naphthalenesulfonate, and urea were obtained from Sigma-Aldrich (USA).

Sample Preparation and Alpha-Glucosidase Activity Assay

Alpha-glucosidase was denatured in solutions containing different concentrations of urea in 50 mM phosphate buffer (pH 6.8) for 2 h at 25 °C. The final concentration of urea was varied from 0 to 6 M. The alpha-glucosidase activity was determined at 37 °C by measuring the change of absorbance at 400 nm that accompanies the hydrolysis of pNPG to generate pNP. The assay system contained 5 mM pNPG in 50 mM phosphate buffer (pH 6.8), and the reaction was stopped by adding a double volume of a 1 M $NaCO_3$ solution. The activity and absorption were measured with a Helios Gamma Spectrophotometer (Thermo Spectronic, UK). A calibration curve was constructed to correlate the absorption change with the generation of pNP. One unit of enzyme activity was defined as the amount of enzyme that liberated 1.0 μM of D-glucose from pNPG per minute at pH 6.8 at 37 °C.

Intrinsic and ANS-Binding Fluorescence Measurements

The samples were treated for 2 h in incubating solutions containing different concentrations of urea at 25 °C. The final enzyme concentration was 2.2 μM. The intrinsic fluorescence spectra were measured with an excitation wavelength of 280 nm, and the emission wavelengths ranged from 300 to 400 nm. These data were recorded with an F-2500 fluorescence spectrophotometer (Hitachi, Japan) using a 1-cm path-length cuvette.

The changes in ANS-binding fluorescence intensity were studied by labeling the samples with 40 μM ANS for 30 min prior to measurement. An excitation wavelength of 380 nm was used for ANS-binding fluorescence, and the emission wavelengths ranged from 400 to 600 nm. After the enzyme sample was incubated with urea for 2 h, 20-fold ANS was added to each sample. The final enzyme concentration was 2.2 μM. All reactions and measurements were carried out in 50 mM phosphate buffer (pH 6.8) at 25 °C.

Aggregation Analysis

Equations were adopted from methods previously reported for the kinetic analysis of CK aggregation [16–18].

$$\Delta AG = AG - AG_t \tag{1}$$

where AG is the absorbance at the end of the aggregation reaction before reaching the precipitation state, and AG_t is the absorbance at time t during aggregation. The experimental data were fitted to a first-order expression as:

$$\Delta AG = \exp(-k_{AG}/t) \tag{2}$$

where k_{AG} is the rate constant for a monophasic reaction.

Homology Modeling of the Alpha-Glucosidase Structure and Docking Simulations

The 3D model of alpha-glucosidase, comprising 584 amino acids (NCBI accession no.: NP_011808.1), was built using MODELLER9v1 [19] based on homology modeling [20]. We retrieved known homologous structures from the Protein Data Bank (PDB) (http://www.pdb.org) and found that the Cereus oligo-1,6-glucosidase (PDB entry: 1UOK) [21] was a suitable structural template (38% sequence identity). A sequence alignment of alpha-glucosidase and the template was constructed by mGenTHREADER in the PSIPRED protein structure prediction server [22]. Based on the sequence alignment, the 3D structure of alpha-glucosidase was constructed with a high level of confidence. We then calculated the conformational energy of the structural model using the Discrete Optimized Protein Energy (DOPE) score as our stability measure. AutoDock4 [23], Dock6 [24], and FlexX [25] are currently widely used for in silico protein-ligand docking. AutoDock uses a stochastic method, and DOCK and FlexX use an incremental construction method [26]. We used all these different programs to predict the docking structure of alpha-glucosidase and urea (PubChem database CID: 1176). The docking preparation procedure steps were (1) converting the structure from 2D to 3D, (2) calculating charges, (3) adding hydrogen atoms, and (4) finding pockets. For these steps, we used OMEGA (http://www.eyesopen.com) and OpenBabel (http://openbabel.sourceforge.org).

Results

Inactivation of Alpha-Glucosidase During Denaturation in a Urea Solution

Alpha-glucosidase was inactivated with various concentrations of urea in a dose-dependent manner (Fig. 1). Because urea has a soft electrophilic property, a relatively high concentration was needed to inactivate the enzyme completely (IC_{50}=3 M). At less than 2 M urea, the activity was still sustained and was drastically decreased when the urea concentration was increased in the range of 2 to 4 M (Fig. 1a). We also checked the reversibility of urea inhibition by examining plots of the remaining activity versus the different concentrations of enzyme at various urea concentrations (Fig. 1b). The results showed straight lines that passed through the origin, indicating that the inactivation by urea was reversible.

Inactivation Kinetics of Alpha-Glucosidase Denatured in Different Urea Solutions

To detect inactivation kinetics and rate constants, we performed time-interval measurements (Fig. 2). The results showed that the enzyme activity gradually decreased in a time-dependent manner with the first-order reaction (Fig. 2a). Subsequent analysis from the semilogarithmic plot showed the monophasic inactivation. The microscopic rate constant was calculated as $k=0.046\pm0.01x$ min^{-1} (Fig. 2b).

For the analysis of a mixed-type inhibition mechanism, the Lineweaver–Burk equation in double reciprocal form can be written as:

$$\frac{1}{v}=\frac{K_{\mathrm{m}}}{V_{\max}}\left[1+\frac{[I]}{K_{\mathrm{i}}}\right]\frac{1}{[S]}+\frac{1}{V_{\max}}\left[1+\frac{[I]}{\alpha K_{\mathrm{i}}}\right] \tag{3}$$

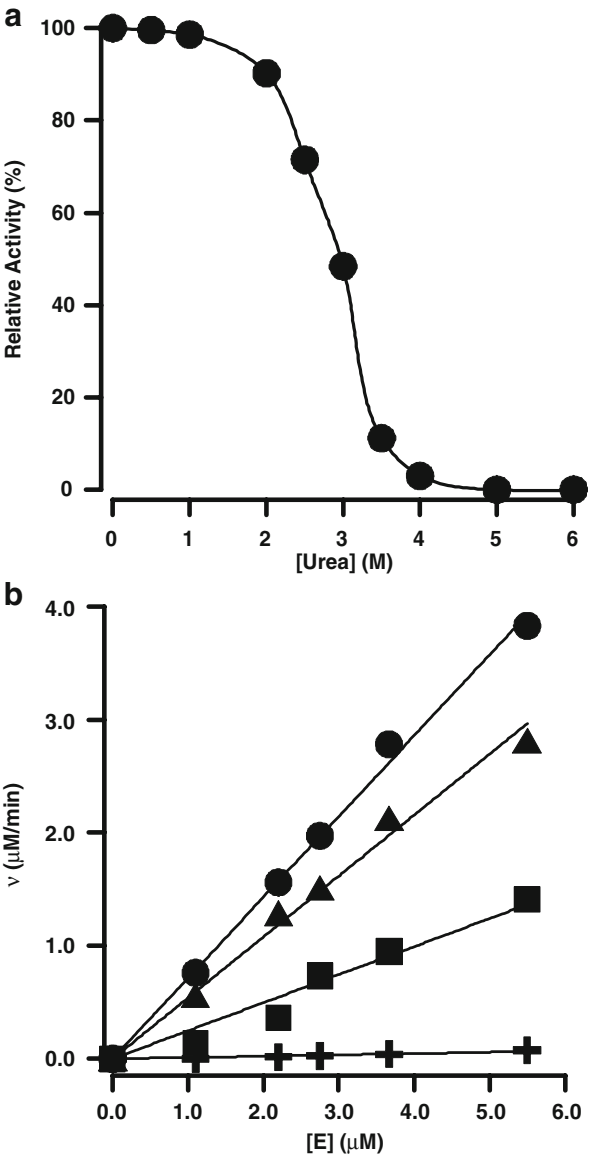

Fig. 1 Effect of urea on the activity of alpha-glucosidase. **a** The enzyme was incubated with urea for 2 h at 25 °C. The activity was then measured with a native control enzyme. The final enzyme concentration was 2.2 μM. Data are presented as mean values (n=3). **b** The plots of v versus [E]. The urea concentrations were 0 (*circles*), 2.5 (*triangles*), 3.5 (*squares*), and 4.0 M (*plus signs*)

Secondary replots can be constructed from

$$\text{Slope} = \frac{K_m}{V_{max}} + \frac{K_m[I]}{V_{max}K_i} \tag{4}$$

and

$$Y - \text{intercept} = \frac{1}{V_{max}^{app}} = \frac{1}{V\text{max}} + \frac{1}{\alpha K_i V_{max}}[I] \tag{5}$$

The secondary replot is linearly fitted in the case of a single inhibition site or a single class of sites. The K_i value can be obtained from the above equations. A plot of slope versus

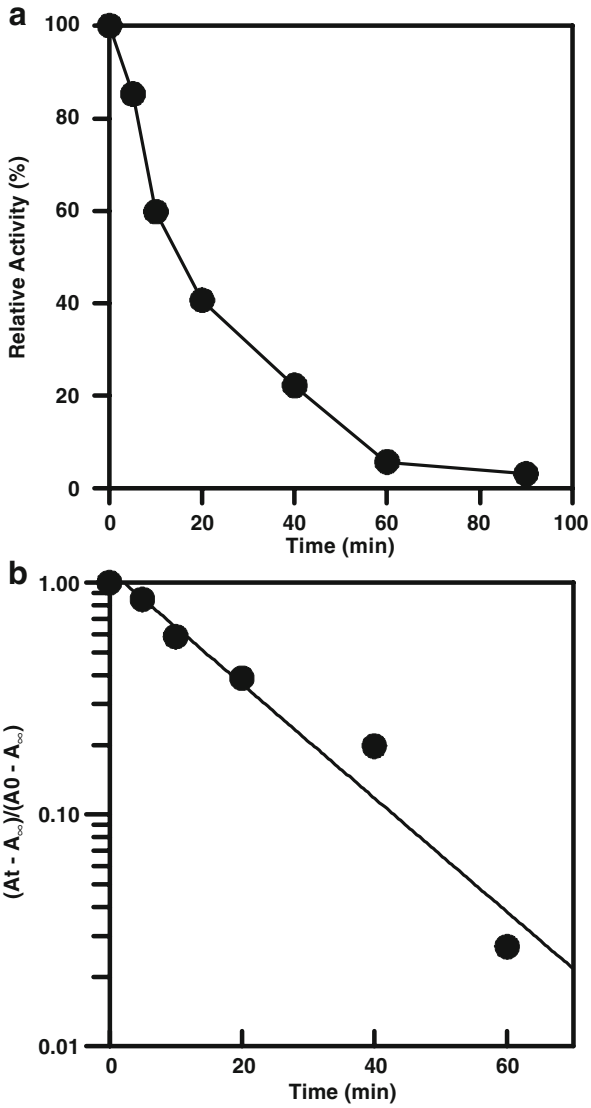

Fig. 2 Kinetic inactivation time-course for alpha-glucosidase in the presence of urea. **a** Time-interval measurement. The final enzyme and urea concentrations were 2.2 μM and 4 M, respectively. **b** A semilogarithmic plot. The data points of the curve were taken from **a**

[*I*] and *Y*-intercept versus [*I*] converts the relationship to a straight line, described as Scheme 1.

A Lineweaver–Burk plot analysis showed that both the apparent K_m and V_{max} changed simultaneously (Fig. 3): The apparent K_m increased while the apparent V_{max} decreased, indicating that a mixed-type of inhibition was induced by urea. By using the data obtained from Fig. 3, α was calculated as 1.17 from the intersection point, and the K_i value was calculated as 1.73 M according to Eqs. 3 to 5; this is matched well to the model of Scheme 1. We hypothesized that urea can directly form a ligand bond with alpha-glucosidase at, near, or inside the active site, which in turn induces a conformational change to inactivate the enzyme. Intuitively, partial conformational changes affect the substrate-

Scheme 1 A scheme

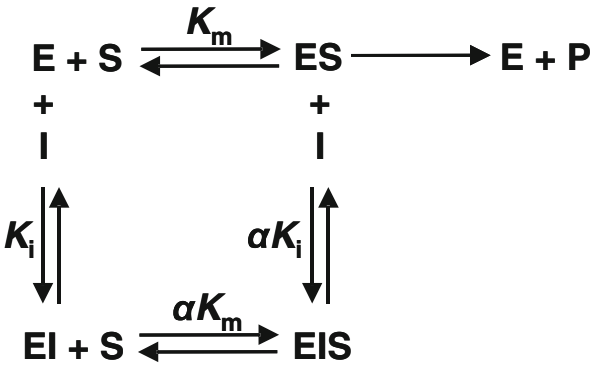

enzyme state with the V_{max} changes, and this may also increase substrate access to the active site.

Conformational Changes of Alpha-Glucosidase During Urea Denaturation

To confirm our hypothesis, we measured the structural changes of alpha-glucosidase in the presence of urea (Fig. 4). From the intrinsic fluorescence spectra results, we observed that urea binding to alpha-glucosidase resulted in conformational changes: The maximum peak significantly red-shifted from 334 to 347 nm in a dose-dependent manner (Fig. 4a). The red-shift of the maximum peak was no longer changed at urea concentrations of 8 M or higher, and this showed a saturated equilibrium binding state between urea and alpha-

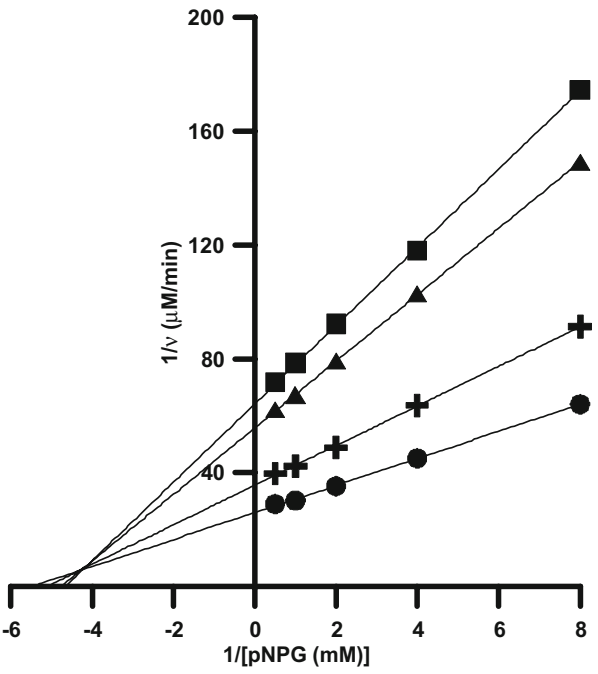

Fig. 3 Lineweaver–Burk plot. The urea concentrations were 0 (*circles*), 2.5 (*triangles*), 2.75 (*plus signs*), and 3 M (*squares*). The enzyme was incubated with urea for 2 h at 25 °C, and then the activity was measured. The final enzyme concentration was 2.2 μM

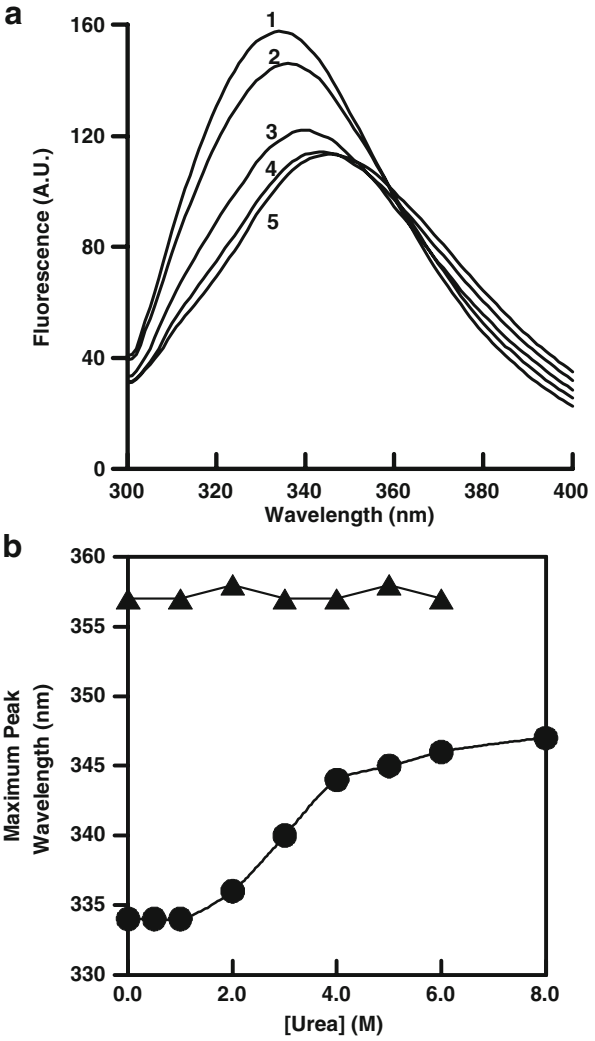

Fig. 4 Intrinsic fluorescence spectra changes of alpha-glucosidase by urea. **a** The enzyme was incubated with different concentrations of urea for 2 h. The final enzyme concentration was 1.1 μM. The excitation wavelength was 280 nm. The urea concentrations for curves *1–5* were 0, 2, 3, 4, and 5 M, respectively. **b** Secondary replot of the maximum wavelength versus urea. *Circles* alpha-glucosidase and *triangles N*-acetyl-tryptophan. The experimental conditions were the same as **a**

glucosidase. The plot of peak wavelength versus urea is displayed in more detail in Fig. 4b; the maximum peak wavelength, which occurred when the urea concentration was higher than 2 M, increased in a urea-dose-dependent manner. For control, *N*-acetyl-tryptophan was used, and the result showed that the maximum peak change was not induced by simple urea interference. At concentrations of urea lower than 2 M, tertiary structural changes did not occur, which is consistent with the inactivation results, which demonstrated that a change in activity did not occur in less than 2 M urea (Fig. 1).

To compare changes in exposure of the hydrophobic surface induced by urea, we measured the ANS-binding fluorescence spectra (Fig. 5). The result of this measurement showed that as the concentration of urea increased, the ANS-fluorescence intensity increased gradually in a dose-dependent manner. In contrast to an intrinsic fluorescence change, the hydrophobic surface was exposed gradually to urea, even under a 2 M concentration, which is different from the intrinsic maximum peak wavelength changes.

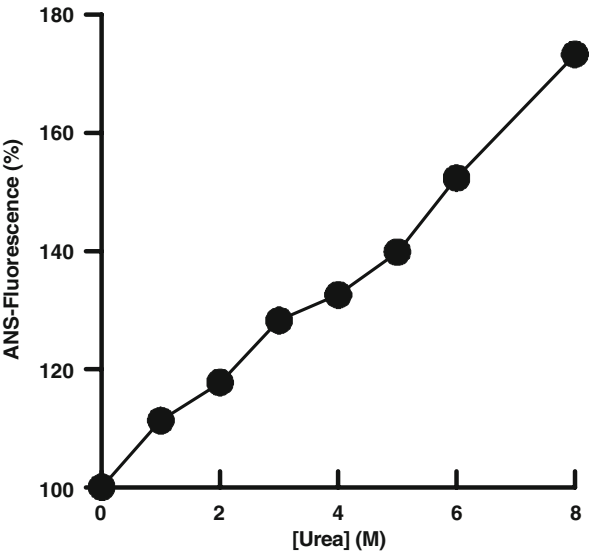

Fig. 5 ANS-binding fluorescence spectra change of alpha-glucosidase by urea. ANS (40 μM) was incubated for 30 min to label the hydrophobic enzyme surface prior to measurement after incubation with urea for 2 h. The final concentration of the enzyme was 1.1 μM. The excitation wavelength was 380 nm

Due to the limited hydrophobic exposure in the presence of less than 2 M urea, this increase did not induce a change in the activity of the enzyme; however, folding intermediates accumulate at this range of urea.

Because hydrophobic surface changes are associated with the active site and conformational changes in the active site do not always change the conformation of the entire enzyme molecule, the ANS-labeled fluorescence change could reflect accumulation of unstable unfolding intermediates at this range of urea concentrations. To affirm our hypothesis, we next tested the aggregation phenomena, which is observed frequently in the folding pathway and competes with correct folding.

Aggregation of Alpha-Glucosidase During Urea Denaturation

When the enzyme was incubated in the presence of urea at 37 °C, we successfully captured the aggregation. As expected, 0.5 M urea induced the most significant aggregation, and with increasing urea concentrations, the aggregation was gradually suppressed. Then, when the concentration of urea reaches 4.0 M, the aggregation disappeared completely (Fig. 6a), indicating that the strong ionic strength resulting from the high concentration of urea unfolded the polypeptide extensively and led the enzyme to form very stable unfolded intermediates. Our subsequent kinetic analyses showed that alpha-glucosidase has a tendency to follow first-order kinetics, and the semilogarithmic plot analysis showed a monophasic process for aggregation (Fig. 6b). The aggregation rate constants (k_{AG}) for 0.5, 2.0, and 3.0 M urea were 0.42, 0.20, and 0.19×10^{-3} s^{-1}, respectively, according to Eqs. 1 and 2.

Comparison of Inactivation and Conformational Changes of Alpha-Glucosidase During Urea Denaturation

To compare changes between activity and conformation, we generated a plot of change ratio versus urea concentration (Fig. 7). The relative activity and the intrinsic

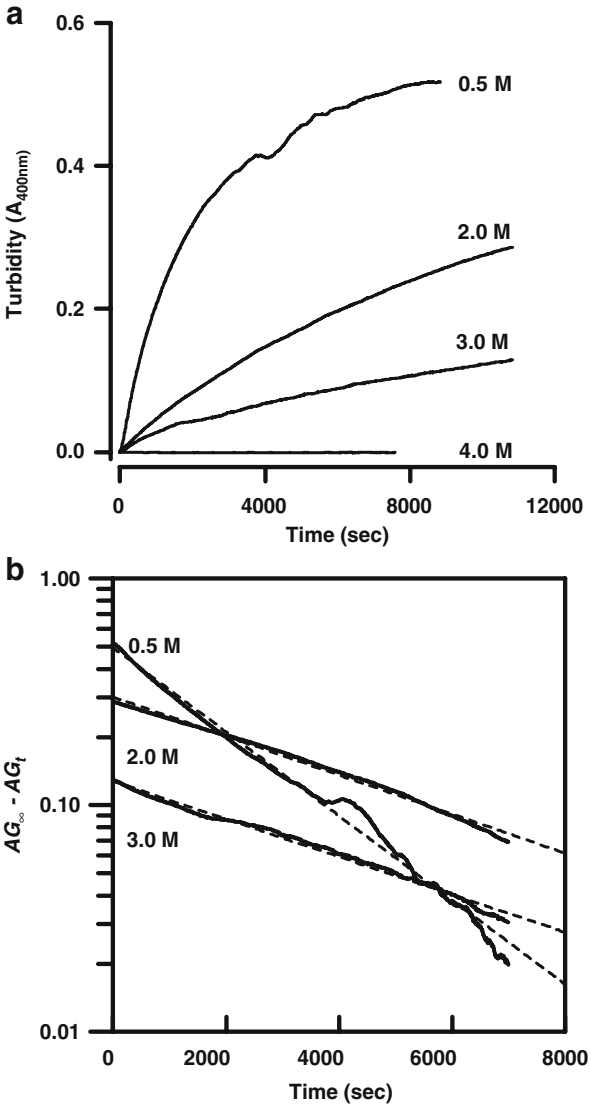

Fig. 6 Aggregation of alpha-glucosidase in the presence of urea. **a** The enzyme was incubated with different concentrations of urea at 37 °C. The labels indicate the final urea concentrations. The final enzyme concentration was 10 μM. **b** A semilogarithmic plot. The data were obtained from **a**

conformational changes synchronized in less than 3 M urea, and the activity change occurred at urea concentrations higher than 3 M. These results showed that the active site is very flexible and is more rapidly inactivated when the overall conformational change has not yet occurred. Both activity and structural changes were completely abolished in the presence of 8 M urea. In contrast, even at urea concentrations less than 3 M urea, disruption of the hydrophobic surface of alpha-glucosidase occurred. This observation consistently supports our supposition that the active site is flexible compared to the overall structure and that the hydrophobic surface at the active site pocket is the area of the protein most altered by urea. Interestingly, at this range of urea concentrations, enzyme aggregation was conspicuously observed as shown in Fig. 6.

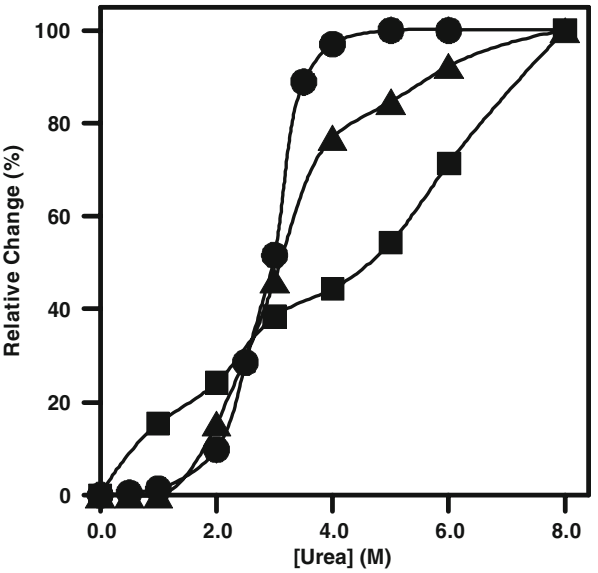

Fig. 7 Comparison of inactivation and unfolding of alpha-glucosidase in the presence of urea. The data were taken from Figs. 1 (*circles*), 4 (*triangles*), and 5 (*squares*)

Computational Modeling and Docking Simulation

After searching for a template for alpha-glucosidase, we selected *Cereus* oligo-1,6-glucosidase (PDB entry: 1UOK) as a template structure and then conducted the sequence alignment. The results showed that although the sequence identity had a relatively low score of 38% when we selected a template structure, the root mean square deviation score of the resulting model was highly significant with a 0.46 Å model structure (Fig. 8a). Also, DOPE scores were virtually the same (alpha-glucosidase: −71906; and 1UOK: -66885), indicating that the model structure was nearly a native structure (Fig. 8b). In the predicted structure of alpha-glucosidase, we found a large binding pocket which expanded to 155 $Å^3$, and the size of this pocket is the second largest in alpha-glucosidase. We detected putative binding sites for urea near this pocket (Fig. 8c). The docking between alpha-glucosidase and urea was successful with significant scores of −3.00 kcal/mol by AutoDock4, −12.68 kcal/mol by DOCK6, and −20.65 kcal/mol by FlexX3. Using the AutoDock4, DOCK6, and FlexX3 results, we searched for urea binding residues of alpha-glucosidase, which were close to a 5-Å distance; the predicted binding residues of alpha-glucosidase are listed in Table 1. When we compared the results from the three different docking programs, several residues were found to commonly interact with urea: THR9, TRP14, LYS15, THR287, ALA289, ASP338, SER339, and TRP340. The results show that docking prediction can be valuable in locating residues involved in agonist binding.

Discussion

Urea disrupted the structure of alpha-glucosidase by interacting with polar peptide linkages and anionic sites. This protein–solute interaction promoted unfolding of the tertiary protein structure into a more energetically favorable state. Urea and guanidine hydrochloride are thought to interact strongly with a protein's charged hydrophilic residues that are situated at the surface of the protein, resulting in swelling of the protein, exposure of hydrophobic


a

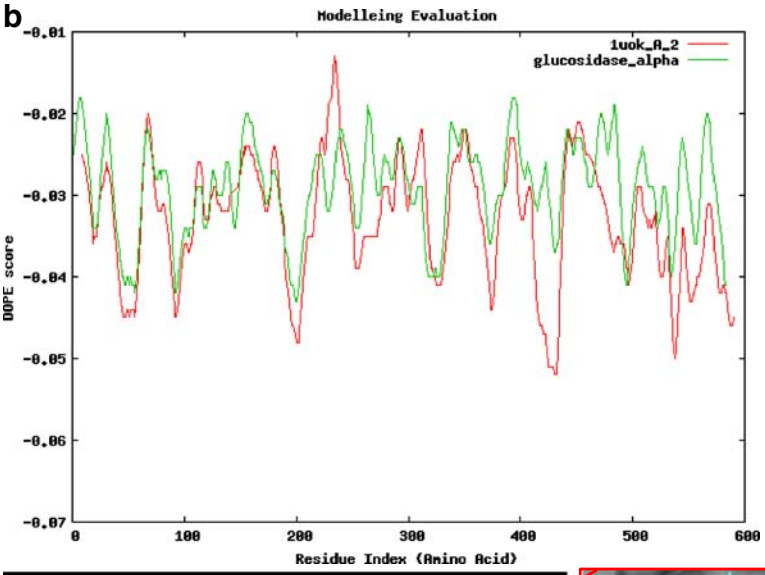
b
Modelleing Evaluation
1uok_A_2
glucosidase_alpha
DOPE score
-0.01
-0.02
-0.03
-0.04
-0.05
-0.06
-0.07
0
100
200
300
400
500
600
Residue Index (Amino Acid)

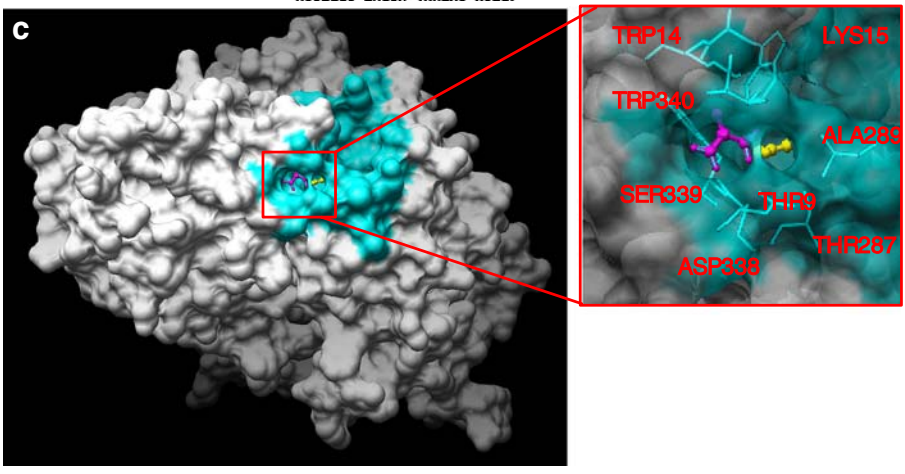
c
TRP14
LYS15
TRP340
ALA289
SER339
THR9
THR287
ASP338

◀ **Fig. 8** Predicted 3D structure of alpha-glucosidase and docking simulation. **a** The urea ligand binding sites of alpha-glucosidase are indicated by *yellow* (DOCK6), *pink* (AutoDOCK4), and *blue colors* (FlexX3). **b** Plot of DOPE score versus residue index. **c** Docking simulation with urea. The *red box* indicates computational docking results for alpha-glucosidase and urea. The colored sticks represent urea: The *yellow stick* was docked by the DOCK6 program, the *pink stick* was docked by AutoDOCK4, and the *blue stick* was docked by FlexX3. The *pink stick* and the *blue stick* piled in the same position

residues, and eventually the penetration of water and denaturant into the core of the protein, followed by unfolding.

Our investigation indicated that different concentrations of urea-induced different folding states of alpha-glucosidase. First, in less than 2 M urea, no changes in the activity or structure of alpha-glucosidase occurred, but we observed exposure of the hydrophobic surface, which may induce aggregation due to hydrophobic interactions. At this range of urea concentrations, unfolding intermediates of alpha-glucosidase prone to aggregate under suitable conditions do accumulate. Second, in the range of 2 to 4 M urea, the activity of the enzyme changed exponentially and all remaining enzymatic activity was almost completely abolished. The enzyme was drastically inactivated according to a first-order monophasic reaction. Simultaneously, there were substantial changes in the tertiary structural of the enzyme, including hydrophobic surface exposure. Third, at the range of 4 to 6 M urea, the aggregation of alpha-glucosidase was completely suppressed due to the strong ionic strength of urea, implying that the enzyme molecules were in a stable form at this range of urea concentrations. Activity was no longer detected as the tertiary structure was extensively unfolded, as monitored by a significant red-shift in the florescence spectra. The hydrophobic surface was still not completely exposed at this stage. Forth, at concentrations higher than 6 M, complete unfolding of alpha-glucosidase occurred. Based on a comparison of the activity and the structural changes in Fig. 7, we determined that a concentration of urea of 3 M urea is the critical turning point based on kinetic parameters (IC_{50} and K_i values). Furthermore, aggregation is significantly suppressed at this concentration.

Table 1 The predicted urea-docking residues of alpha-glucosidase (<5 Å distance).

Amino acids	No. of residues		
	Autodock4	FlexX3	Dock6
HIS	6	6	–
PRO	7	7	–
GLU	8	8	–
THR	9	9	9
GLU	10	10	–
TRP	14	14	14
LYS	15	15	15
THR	287	287	287
SER	–	–	288
ALA	289	289	289
SER	–	–	295
ILE	334	334	–
THR	337	337	–
ASP	338	338	338
SER	339	339	339
TRP	340	340	340

To the best of our knowledge, our study is the first to simulate the 3D structure of alpha-glucosidase. Because homology modeling is based on the premise that evolutionarily related proteins share a similar structure, the accuracy of structural prediction depends strongly on the pairwise sequence identity between a query sequence and a template structure. The computational docking simulation suggested several docking sites for urea; urea is apparently easily buried in the inside of the pocket. For the urea to interact with the enzyme molecule at the active site initially, partial unfolding is required. In this regard, our computational simulations support our experimental finding that urea concentrations higher than 2 M begin to inactivate enzyme activity. Our conditions only simulated the equilibrium docking state between urea and alpha-glucosidase; the dynamic state where small molecules can access the inner part of the enzyme molecule during unfolding was not observed. The urea-docking sites predicted in this study are located mostly inside and near the pocket; however, this location prediction only occurred at the regional part prior to unfolding. The docking sites that become available after unfolding induced by a high urea concentration (>2 M) were obscure under our conditions.

Finally, we propose an unfolding pathway for alpha-glucosidase from *S. cerevisiae* (Scheme 2).

In Scheme 2, N is the native state, and U_I and $U_I^{/}$ are the partially inactivated and unfolded intermediate states, respectively. U is an extensively unfolded state, and k and k_{AG} are the kinetic first-order rate constants for inactivation and aggregation processes, respectively. Kinetic transient intermediates were split into two states, U_I and $U_I^{/}$, followed by an increasing denaturant concentration, showing that intermediate (U_I) was populated in the presence of a rather high concentration of denaturant in the unfolding pathways; these appeared in real-time analysis with a k first-order rate constant. The kinetic real-time analyses for inactivation and aggregation reflect the presence of transient intermediate states. Aggregation was probably caused by the accumulation of intermediates with urea-exposed hydrophobic surfaces that competed with correct unfolding. Disruption of the noncovalent bond by denaturants occurred very rapidly and was accompanied by a loss of most of the enzymatic activity; the enzyme then underwent complete unfolding. Intermediate accumulation also indicates that in some respects, alpha-glucosidase has a stable tertiary structure.

In conclusion, urea binding to and inactivation of alpha-glucosidase was studied, and the existence of various unfolded states was revealed. To elucidate the folding mechanism of alpha-glucosidase, we used a combined strategy of inhibition kinetics experiments and computational docking prediction. Our computational prediction analysis provided important 3D structural information for alpha-glucosidase and its interaction with urea

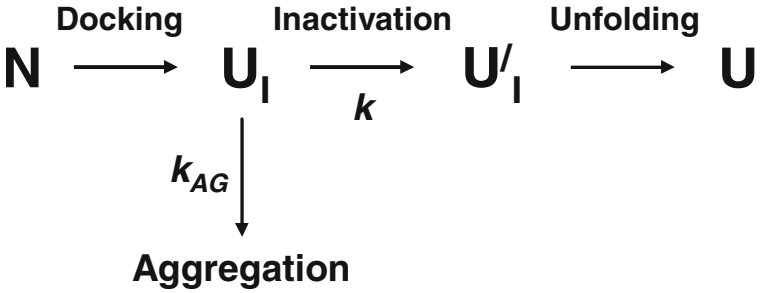

Scheme 2 An unfolding pathway for alpha-glucosidase from *S. cerevisiae*

and predicted amino acid residues in the active pocket of alpha-glucosidase that are involved in the urea-induced unfolding of this enzyme.

Acknowledgements Dr. Fei Zou was supported by a grant from the National Basic Research Program of China (no. 2006CB504100). Dr. Jong Bhak was supported by a grant from the KRIBB Research Initiative Program of Korea. Dr. Yong-Doo Park was supported by fund from the Science and Technology Planning Project of Jiaxing (no. 2008AZ1024), Zhejiang.

References

1. Charron, M. J., Dubin, R. A., & Michels, C. A. (1986). *Molecular and Cellular Biology, 6*, 3891–3899.
2. Kuriki, T., & Imanaka, T. (1999). *Journal of Bioscience and Bioengineering, 87*, 557–565. doi:10.1016/S1389-1723(99)80114-5.
3. Noguchi, A., Nakayama, T., Hemmi, H., & Nishino, T. (2003). *Biochemical and Biophysical Research Communications, 304*, 684–690. doi:10.1016/S0006-291X(03)00647-8.
4. Jespersen, H. M., MacGregor, E. A., Henrissat, B., Sierks, M. R., & Svensson, B. (1993). *Journal of Protein Chemistry, 12*, 791–805. doi:10.1007/BF01024938.
5. Godbout, A., & Chiasson, J. L. (2007). *Current Diabetes Reports, 7*, 333–339. doi:10.1007/s11892-007-0055-x.
6. Scheen, A. J. (2003). *Drugs, 63*, 933–951. doi:10.2165/00003495-200363100-00002.
7. Wehmeier, U. F., & Piepersberg, W. (2004). *Applied Microbiology and Biotechnology, 63*, 613–625. doi:10.1007/s00253-003-1477-2.
8. Moosavi-Movahedi, A. A., & Nazari, K. (1995). *International Journal of Biological Macromolecules, 17*, 43–47. doi:10.1016/0141-8130(95)93517-2.
9. Zou, Q., Habermann-Rottinghaus, S. M., & Murphy, K. P. (1998). *Proteins, 31*, 107–115. doi:10.1002/(SICI)1097-0134(19980501)31:2<107::AID-PROT1>3.0.CO;2-J.
10. Shemer, A., Nathansohn, N., Kaplan, B., Weiss, G., Newman, N., & Trau, H. (2000). *International Journal of Dermatology, 39*, 532–534. doi:10.1046/j.1365-4362.2000.00986-3.x.
11. Hagemann, I., & Proksch, E. (1996). *Acta Dermato-Venereologica, 76*, 353–356.
12. Savica, S., Tamburic, S., Savic, M., Cekic, N., Milic, J., & Vuleta, G. (2004). *International Journal of Pharmaceutics, 271*, 269–280. doi:10.1016/j.ijpharm.2003.11.033.
13. do Couto, S. G., Oliveira Mde, S., & Alonso, A. (2005). *Biophysical Chemistry, 116*, 23–31. doi:10.1016/j.bpc.2005.01.009.
14. Lodén, M., Andersson, A. C., Andersson, C., Frödin, T., Oman, H., & Lindberg, M. (2001). *Skin Research and Technology, 7*, 209–213. doi:10.1034/j.1600-0846.2001.070401.x.
15. Peck, K. D., Ghanem, A. H., & Higuchi, W. I. (1995). *Journal of Pharmaceutical Sciences, 84*, 975–982. doi:10.1002/jps.2600840813.
16. Hahn, H. S., Park, Y. D., Lee, J. R., Park, K. H., Kim, T. J., Yang, J. M., et al. (2003). *Journal of Protein Chemistry, 22*, 563–570. doi:10.1023/B:JOPC.0000005506.98513.43.
17. Zou, H. C., Yu, Z. H., Wang, Y. J., Yang, J. M., Zhou, H. M., Meng, F. G., et al. (2007). *Journal of Biomolecular Structure & Dynamics, 24*, 359–368.
18. Zou, H. C., Lü, Z. R., Wang, Y. J., Zhang, Y. M., Zou, F., & Park, Y. D. (2009). *Applied Biochemistry and Biotechnology, 152*, 15–28. doi:10.1007/s12010-008-8282-4.
19. John, B., & Sali, A. (2003). *Nucleic Acids Research, 31*, 3982–3992. doi:10.1093/nar/gkg460.
20. Rodriguez, R., Chinea, G., Lopez, N., Pons, T., & Vriend, G. (1998). *Bioinformatics (Oxford, England), 14*, 523–528. doi:10.1093/bioinformatics/14.6.523.
21. Watanabe, K., Hata, Y., Kizaki, H., Katsube, Y., & Suzuki, Y. (1997). *Journal of Molecular Biology, 269*, 142–153. doi:10.1006/jmbi.1997.1018.
22. Bryson, K., McGuffin, L. J., Marsden, R. L., Ward, J. J., Sodhi, J. S., & Jones, D. T. (2005). *Nucleic Acids Research, 33*, W36–W38. doi:10.1093/nar/gki410.
23. Morris, G. M., Goodsell, D. S., Halliday, R. S., Huey, R., Hart, W. E., Belew, R. K., et al. (1998). *Journal of Computational Chemistry, 19*, 1639–1662. doi:10.1002/(SICI)1096-987X(19981115)19:14<1639::AID-JCC10>3.0.CO;2-B.
24. Moustakas, D. T., Lang, P. T., Pegg, S., Pettersen, E., Kuntz, I. D., Brooijmans, N., et al. (2006). *Journal of Computer-Aided Molecular Design, 20*, 601–619. doi:10.1007/s10822-006-9060-4.
25. Rarey, M., Kramer, B., Lengauer, T., & Klebe, G. (1996). *Journal of Molecular Biology, 261*, 470–489. doi:10.1006/jmbi.1996.0477.
26. Moitessier, N., Englebienne, P., Lee, D., Lawandi, J., & Corbeil, C. R. (2008). *British Journal of Pharmacology, 153*, S7–S26. doi:10.1038/sj.bjp.0707515.